A Baroclinic Model of the Atmosphere Applicable to the Problem of Numerical Forecasting in Three Dimensions.[1] II.

By G. ÁRNASON, University of Stockholm

(Manuscript received July 5, 1952. Revised manuscript received February 4, 1953)

Abstract

A theory for the application to numerical forecasting of a 3-parameter model of the troposphere is developed and then tested on one synoptic case. The model itself has been described in an earlier paper. An essential feature of this model, beyond other models so far introduced, is that the static stability may vary arbitrarily in a horizontal direction and with time as well. This implies a thermal wind which may change direction with height, and it is shown that this non-parallelism of the isotherms in the vertical is important from the standpoint of thermodynamics. Furthermore, it is shown that the rotation of the thermal wind with height is closely connected with cyclogenesis and the deepening and filling of existing cyclones.

The case selected for numerical computation was the synoptic situation of November 24, 1951, at 03z over Western Europe and the easternmost part of the Atlantic. Tendencies for sea level pressure and for the two parameters defining the tropospheric temperature distribution with height were computed; they compared fairly well with observed changes.

Introduction

In a previous paper, published in the November 1952 number of Tellus, the writer introduced a four-parameter model of the atmosphere, ÁRNASON (1952). This model was based upon the observed characteristics of the distribution of temperature with height; namely, that the atmosphere is divided into a troposphere and a stratosphere, both of which show approximately constant lapse-rate in the vertical. It was found that three parameters were needed to account for the main features of the observed temperature distribution; those selected were the following: sea level temperature (of the model) τ_0, the tropospheric temperature lapse-rate k (independent of height) and the height h of the tropopause. In order to describe the vertical distribution of pressure one more parameter was needed, and the sea level pressure p_0 was chosen.

Regarding the details of the model, the reader is directed to the paper quoted above, which in this article will be referred to as part I.

The main application of this model in I was an integration of the vorticity equation with regard to height followed by some discussion of the resulting two-dimensional equation. Two levels of particular interest to numerical forecasting, namely the levels of mean wind and non-divergence were discussed in some detail by means of the integrated vorticity equation. Certain valuable information regarding the heights of these two levels was gained.

The present paper is a continuation of I and is devoted to the application of the model to numerical forecasting of the fields of temperature and pressure in the troposphere. Some use is made of the information gained in I regarding the two important levels mentioned above. A forecast for the stratosphere has not been attempted in this our first approach toward three-dimensional forecasting, and

[1] This work has been made possible by a grant from Naturvetenskapliga Forskningsrådet, Stockholm.

this reduces the number of parameters to three; the tropopause height h is not required in this case.

Clearly three prognostic equations are needed in order to predict the future values of the three parameters τ_0, k, and p_0. We assume that the thermodynamics of the model are described with sufficient accuracy by the adiabatic equations, which then can be considered as a prognostic equation for τ_0 and k. A drawback is the appearance of a new unknown quantity, the vertical velocity; however, the boundary condition $w = 0$ at $z = 0$ applied to the adiabatic equation provides us with a prognostic equation without a vertical velocity term.

It was shown in I that the vorticity equation can be written as follows:

$$\varrho \left[\frac{\partial \eta}{\partial t} + \mathbf{v} \cdot \nabla \eta\right] = \eta^2 \frac{\partial}{\partial z}\left(\frac{\varrho w}{\eta}\right) \quad (1, 1)$$

At the level of non-divergence both sides of (1.1) are zero. It is common in methods for numerical forecasting to take advantage of this by integrating the resulting barotropic equation to obtain height tendencies. In our case we make use of the fact that the right hand side of (1.1) is zero at this particular level. It is shown in the next section that this piece of information makes it possible to get rid of the vertical velocity in the adiabatic equation when the latter is applied to the level of non-divergence. This results in a second prognostic equation essentially derived from the thermodynamics.

In practice, the level of non-divergence is approximated by a surface $p = \text{const.}$ or a plane $z = \text{const.}$ It is conceivable that the dynamics and the thermodynamics may react differently for this approximation. From repeated integration of the barotropic equation one has gathered a considerable amount of experience as far as the dynamics are concerned. To the authors knowledge, however, this is the first time this approximation has been introduced explicitly in the thermodynamics. Judging from the single case of application to numerical forecasting dealt with in this paper, it would seem that the thermodynamics might be less sensitive than the dynamics for this approximation.

The remaining problem, to find a prognostic equation for p_0, could be solved in different ways, but use will have to be made of the vorticity equation. The most convenient way seems to be to compute the height tendency of the 500 mb level, or another upper level, as an auxiliary quantity and then make use of the hydrostatic equation for finding $\frac{\partial p_0}{\partial t}$. Methods so far designed for the purpose of numerical forecasting have mainly dealt with the forecast of the 500 mb height; several methods exist. Some authors make use of the barotropic vorticity equation, FJØRTOFT (1952), THOMPSON (1952); others, EADY (1952), ELIASSEN (1952), have preferred to solve an integrated (with respect to height) version of the vorticity equation. The latter alternative is used in this paper.

The temperature lapse-rate, k, of the model is a function of the horizontal coordinates; this implies that the isotherms may change direction with height. This non-parallelism turns out to be important from the standpoint of thermodynamics and contributes essentially to the vertical velocity when the latter is determined from the adiabatic equation. Moreover, this change in direction of the isotherms with height has bearing upon cyclogenesis and the filling or deepening of existing cyclones. These aspects are discussed in some detail in the latter half of section 2. The main results are that, *advection of lower lapse-rate favours pressure falls (cyclogenesis, deepening) and advection of higher lapse-rate favours pressure rises (filling of a cyclone, intensification of an anticyclone)*. Moreover, ascending motion is intimately connected with warm air advection and descending motion intimately connected with cold air advection.

Section 3 deals with the predicted tendencies of p_0, τ_0, and k for the synoptic situation of Nov. 24, 1951 at 03 z over Western Europe and the Eastern Atlantic. By and large the forecast is successful. The prediction of sea level pressure is fairly good but suffers somewhat from a poor 500 mb forecast in certain areas. The importance of the non-parallelism of the isotherms with height shows up clearly in the numerical forecast and this effect partially explains the sudden deepening of an old cyclone off the Norwegian coast.

2. Theory for the application to numerical forecasting

The prognostic equations. When applied to the tropospheric part of the model, the adiabatic equation may be written as follows:

$$\frac{\partial \tau_0}{\partial t} - z\,\frac{\partial k}{\partial t} + \mathbf{v}\cdot\nabla\tau + sw - \frac{1}{c_p\varrho}\,\frac{\partial p}{\partial t} = 0 \qquad (2,\ 1)$$

Here $s = k_a - k$ and is an expression for the static stability, where k_a denotes the adiabatic lapse-rate and k the actual one, c_p is the specific heat of the air at constant pressure, and $\mathbf{v}$ is the geostrophic wind. From I, (2, 3) and (2, 12), we obtain the following expression for the advection term $\mathbf{v}\cdot\nabla\tau$:

$$\mathbf{v}\cdot\nabla\tau = \frac{\tau}{\tau_0}\,\mathbf{v}_0\cdot\nabla\tau_0 - \frac{\tau}{\tau_0}\,z\,\mathbf{v}_0\cdot\nabla k - \frac{z^2}{2}\,\mathbf{v}'\cdot\nabla k \qquad (2,\ 2)$$

when the conditions $\mathbf{v}'\cdot\nabla\tau_0 = \mathbf{v}''\cdot\nabla k = 0$ and $\mathbf{v}''\cdot\nabla\tau_0 = -\frac{1}{2}\,\mathbf{v}'\cdot\nabla k$ have been utilized.

At the lower boundary $z = 0$, we assume $w = 0$, and equ. (2, 1) is there reduced to:

$$\frac{\partial \tau_0}{\partial t} + \mathbf{v}_0\cdot\nabla\tau_0 - \frac{1}{c_p\varrho_0}\,\frac{\partial p_0}{\partial t} = 0 \qquad (2,\ 3)$$

Equ. (2, 3) is the first prognostic equation; it renders a relationship between the time derivatives of two of the parameters and does not contain other unknown quantities. The last term is in general considerably smaller than either of the other terms, and $\frac{\partial \tau_0}{\partial t}$ is therefore essentially determined by the advection term $\mathbf{v}_0\cdot\nabla\tau_0$. The latter is computed from the charts for p_0 and τ_0.

The next prognostic equation will be derived by making use of the assumption that we know the height of the level of non-divergence. At this particular level the following condition applies (see 1,1):

$$\frac{\partial}{\partial z}\left(\frac{\varrho w}{\eta}\right) = 0 \qquad (2,\ 4)$$

By means of this equation the vertical velocity can be eliminated from (2, 1). We multiply the latter by ϱ/η and differentiate with respect to z. At the level of non-divergence the vertical velocity term drops out because of (2, 4), and we arrive at the following equation:

$$\frac{\partial}{\partial z}\left(\frac{\varrho z}{\eta}\right)\frac{\partial k}{\partial t} - \frac{\partial}{\partial z}\left(\frac{\varrho}{\eta}\mathbf{v}\cdot\nabla\tau\right) - \frac{\partial}{\partial z}\left(\frac{\varrho}{\eta}\right)\frac{\partial \tau_0}{\partial t} + \frac{1}{c_p}\,\frac{\partial}{\partial z}\left(\frac{1}{\eta}\,\frac{\partial p}{\partial t}\right) = 0 \qquad (2,\ 5)$$

In deriving (2, 5), variation with height of the static stability s has been disregarded. In carrying out the differentiation of the various terms of (2, 5), we will make use of (2, 2), (2, 3) and the hydrostatic equation. Applied to the troposphere of the model, the hydrostatic equation, when integrated with respect to height, takes the form:

$$\frac{1}{\varrho}\,\frac{\partial p}{\partial t} = \frac{\tau}{\varrho_0\tau_0}\,\frac{\partial p_0}{\partial t} + \frac{g}{\tau_0}\,z\left(\frac{\partial \tau_0}{\partial t} - \frac{z}{2}\,\frac{\partial k}{\partial t}\right) \qquad (2,\ 6)$$

The details of the differentiation and rearrangement of the different terms in (2, 5) will not be given here. Rather lengthy computations result in the following relation between the time derivatives $\frac{\partial k}{\partial t}$ and $\frac{\partial p_0}{\partial t}$ of two of the three parameters:

$$\begin{aligned}
&\left[1 - \hat{z}\left(a_1 + \frac{1}{\eta}\,\frac{\partial\eta}{\partial z}\right) + \hat{z}^2\cdot a_2\left(a_3 + \frac{1}{\eta}\,\frac{\partial\eta}{\partial z}\right)\right]\frac{\partial k}{\partial t} + \\
&+ \frac{s_d}{c_p\varrho_0}\left[\frac{1}{\tau} - \frac{\hat{z}}{\tau_0}\left(a_3 + \frac{1}{\eta}\,\frac{\partial\eta}{\partial z}\right)\right]\frac{\partial p_0}{\partial t} = \\
&= \left[\frac{s_d}{\tau} - \frac{\hat{z}}{\tau_0}\left(a_4 + s_d\,\frac{1}{\eta}\,\frac{\partial\eta}{\partial z}\right)\right]\mathbf{v}_0\cdot\nabla\tau_0 - \\
&- \left[1 - \hat{z}\left(a_5 + \frac{\tau}{\tau_0}\,\frac{1}{\eta}\,\frac{\partial\eta}{\partial z}\right)\right]\mathbf{v}_0\cdot\nabla k - \\
&- \hat{z}\left[1 - \frac{\hat{z}}{2}\left(a_6 + \frac{1}{\eta}\,\frac{\partial\eta}{\partial z}\right)\right]\mathbf{v}'\cdot\nabla k
\end{aligned} \qquad (2,\ 7)$$

where $\hat{z}$ is the height of the level of non-divergence and $s_d = \frac{g}{c_p} - k$, i.e. the difference between the dry-adiabatic lapse-rate and the lapse-rate k of the model. The quantities $a_1 \ldots a_6$ have the following meaning:

$$a_1 = \frac{1}{\tau}\left(\frac{g}{R} + s_d\right); \quad a_2 = \frac{g}{2\, c_p \tau_0};$$

$$a_3 = \frac{g}{R\tau}; \quad a_4 = \frac{g}{c_p} a_3; \quad a_5 = \frac{1}{\tau_0}\left(\frac{g}{R} + k\right);$$

$$a_6 = \frac{1}{\tau}\left(\frac{g}{R} - k\right) \qquad (2, 8)$$

After inserting reasonable values for the different quantities composing the coefficients of (2, 7), it becomes obvious that the term with $\frac{\partial p_0}{\partial t}$ can safely be neglected. This means that the only unknown quantity in (2, 7) is $\frac{\partial k}{\partial t}$.

Equation (2, 7) is our second prognostic equation.

The advection terms appearing on the right hand side of (2, 7) are all determinable from the charts for p_0, τ_0 and k. Moreover, the variations in k, τ and τ_0 are of such minor importance to the value of the coefficients in this equation, that for practical purposes mean values will give sufficient accuracy. We have chosen $k = 6.5°$ C/km, $\tau_0 = 285°$, $\tau = 253$, and the following values for $a_1 \ldots a_6$ are obtained: $a_1 = 1.52 \cdot 10^{-4}$, $a_2 = 0.175 \cdot 10^{-4}$, $a_3 = 1.38 \cdot 10^{-4}$, $a_4 = 1.38 \cdot 10^{-6}$, $a_5 = 1.45 \cdot 10^{-4}$ and $a_6 = 1.12 \cdot 10^{-4}$.

Inserting these values into (2, 7) and neglecting the term with $\frac{\partial p_0}{\partial t}$, this equation becomes:

$$\left[1 - \hat{z} \cdot 10^{-4}\left(1.52 + \frac{1}{\eta}\frac{\partial \eta}{\partial z} \cdot 10^4\right) + \right.$$

$$\left. + 0.175 \cdot \hat{z}^2 \cdot 10^{-8}\left(1.38 + \frac{1}{\eta}\frac{\partial \eta}{\partial z} \cdot 10^4\right)\right]\frac{\partial k}{\partial t} =$$

$$= 0.138 \cdot 10^{-4}\left[1 - 0.89 \cdot \hat{z} \cdot 10^{-4} \cdot \right.$$

$$\left. \cdot \left(3.95 + \frac{1}{\eta}\frac{\partial \eta}{\partial z} \cdot 10^4\right)\right] \mathbf{v}_0 \cdot \nabla \tau_0 -$$

$$- \left[1 - 0.89\, \hat{z} \cdot 10^{-4}\left(1.63 + \frac{1}{\eta}\frac{\partial \eta}{\partial z} \cdot 10^4\right)\right] \cdot$$

$$\cdot \mathbf{v}_0 \cdot \nabla k - \hat{z}\left[1 - 0.5\, \hat{z} \cdot 10^{-4} \cdot \right.$$

$$\left. \cdot \left(1.12 + \frac{1}{\eta}\frac{\partial \eta}{\partial z} \cdot 10^4\right)\right] \mathbf{v}' \cdot \nabla k$$

$$(2, 9)$$

It appears from this equation that the term $\frac{1}{\eta}\frac{\partial \eta}{\partial z}$ can be neglected only if it is considerably less than 10^{-4} m^{-1}. This is certainly not the case in general. For instance, a relative change of 35 % in η from the earths surface up to 5 km is presumably not uncommon; this corresponds to an average value of $0.70 \cdot 10^{-4}$ m^{-1} for $\frac{1}{\eta}\frac{\partial \eta}{\partial z}$.

For positive values of $\frac{1}{\eta}\frac{\partial \eta}{\partial z}$ the coefficient for $\frac{\partial k}{\partial t}$ may become zero; in case of $\hat{z} = 5$ km and $k = 6.5°$ C/km, the critical value for $\frac{1}{\eta}\frac{\partial \eta}{\partial z}$ is $0.64 \cdot 10^{-4}$ m^{-1}.

The term $\frac{1}{\eta}\frac{\partial \eta}{\partial z}$ in the equ. (2, 7) and (2, 9) refers to the level $z = \hat{z}$, η and $\frac{\partial \eta}{\partial z}$ are to be computed from the respective equations:

$$(\eta)_{z=\hat{z}} = f + \frac{\tau}{f \varrho_0 \tau_0} \nabla^2 p_0 +$$

$$+ \frac{g}{f \tau_0}\hat{z}\left(\nabla^2 \tau_0 - \frac{\hat{z}}{2}\nabla^2 k\right) \quad (2, 10)$$

$$\left(\frac{\partial \eta}{\partial z}\right)_{z=\hat{z}} = \frac{g}{f\tau_0}(\nabla^2 \tau_0 - \hat{z}\nabla^2 k) =$$

$$= \frac{g}{f\tau_0}(\nabla^2 \tau)_{z=\hat{z}} \qquad (2, 11)$$

In the computation of $(\eta)_{z=\hat{z}}$ and $\left(\frac{\partial \eta}{\partial z}\right)_{z=\hat{z}}$ it is sufficient to use mean values for τ_0 and τ.

The two prognostic equations (2, 3) and (2, 9) contain the three unknown tendencies $\frac{\partial p_0}{\partial t}$, $\frac{\partial \tau_0}{\partial t}$, and $\frac{\partial k}{\partial t}$. In order to produce the third prognostic equation, we will have to make use of the vorticity equation in one form or another. In the derivation of the second prognostic equation, a knowledge of the height of the level of non-divergence was assumed, and it would therefore seem logical to make a barotropic tendency computation for this level. It is quite clear from hydrostatic consideration that the knowledge of the height tendency at this level would provide us with the third and last prognostic equation (see for inst. (2, 6)). It has, however, to be realized that the assumption made in connection with the thermodynamics does not necessarily have to be applied when dealing with the dynamics. Nothing prevents us from making a height tendency computation which should improve on that of the barotropic case. The integrated vorticity equation

$$\frac{\partial \bar{\eta}}{\partial t} + \mathbf{v} \cdot \nabla \bar{\eta} + \gamma\, \mathbf{v}_T \cdot \nabla \zeta_T = 0 \quad (2, 12)$$

derived in part I of this paper will probably yield such an improved forecast. It is to be applied to the level of mean wind as indicated by the bars, and the quantities $\mathbf{v}_T$ and ζ_T mean the thermal wind and thermal vorticity for the layer between this level and sea level. In our model the constant γ is to be put equal to 0.6.

It still is an open question what levels should be chosen to represent the surfaces of non-divergence and mean wind. A study, in part I, of the vorticity equation integrated with respect to height gave the result that in our model the height of the former was in general somewhat above that of the 500 mb surface, whereas the latter was somewhat below. For practical reasons it is therefore tempting to let the 500 mb surface represent both levels in the numerical computations. This is, however, not necessary, since the advection terms (Jacobians) occurring in the vorticity equation and the other prognostic equations are known functions of height. As a suggestion, the 4 and 6 km levels respectively could replace the two surfaces in question.

It is, however, not our intention to give a detailed discussion on this particular matter nor to comment further on the relative merits of different methods of computing height or pressure tendencies at some upper level. We assume that such a tendency computation has been carried out by means of the vorticity equation in one form or another. This implies that we assume the left hand side of (2, 6) p. 000 to be known for a certain z = const. or p = const., and that this equation thereby renders a new relationship between the three tendencies to be determined. Substituting for $\frac{1}{\varrho}\frac{\partial p}{\partial t}$ in (2, 6) from the hydrostatic equation

$$\frac{1}{\varrho}\frac{\partial p}{\partial t} = g\frac{\partial H}{\partial t} \quad (2, 13)$$

and for $\frac{\partial \tau_0}{\partial t}$ from (2, 3), our *third prognostic equation* takes the form:

$$\frac{1}{g\varrho_0}\left[1 + \frac{s_d}{\tau_0}H\right]\frac{\partial p_0}{\partial t} = \frac{H^2}{2\,\tau_0}\frac{\partial k}{\partial t} + \frac{\partial H}{\partial t} + \frac{H}{\tau_0}\mathbf{v}_0 \cdot \nabla \tau_0 \quad (2, 14)$$

where H is the height of the pressure surface, the tendency of which is assumed to be known. Putting $H = 5$ km, $\tau_0 = 285°$ absolute and $\frac{1}{\varrho_0} = 818$, we obtain:

$$\frac{\partial p_0}{\partial t} = 5.0\frac{\partial k}{\partial t} + 1.1\frac{\partial H}{\partial t} + 2.0\,\mathbf{v}_0 \cdot \nabla \tau_0 \quad (2, 15)$$

where p_0, k and H are expressed in mbs, °C km^{-1}, and dekameters respectively. All the terms on the right hand side are of the same order of magnitude, but near fronts and in cold air outbreaks the last term may dominate. A more detailed discussion of this equation will be given later in connection with a discussion of deepening and filling of sea level cyclones.

The vertical velocity. Since the three tendencies $\frac{\partial p_0}{\partial t}$, $\frac{\partial \tau_0}{\partial t}$ and $\frac{\partial k}{\partial t}$ can be computed from the prognostic equations (2, 3), (2, 7) and (2, 14), the vertical velocity is the only unknown in the adiabatic equation (2, 1). Utilizing the equations (2, 2), (2, 3) and (2, 6), we arrive at the following expression for the vertical velocity:

$$sw = z\left[\frac{\partial k}{\partial t} + \mathbf{v}_0 \cdot \nabla k - \right.$$
$$\left. - \frac{s_d}{\tau_0}\left(\mathbf{v}_0 \cdot \nabla \tau_0 - \frac{1}{c_p \varrho_0}\frac{\partial p_0}{\partial t}\right)\right]$$
$$+ z^2\left[\frac{1}{2}\mathbf{v}' \cdot \nabla k - \frac{k}{\tau_0}\mathbf{v}_0 \cdot \nabla k - \frac{g}{2 c_p \tau_0}\frac{\partial k}{\partial t}\right] \quad (2, 16)$$

The term containing $\frac{\partial p_0}{\partial t}$ can safely be neglected, and for our purposes the simplified equation

$$sw = z\left(\frac{\partial k}{\partial t} + \mathbf{v}_0 \cdot \nabla k\right) + \frac{z^2}{2}\mathbf{v}' \cdot \nabla k \quad (2, 17)$$

will give sufficiently accurate results.

The static stability s of an ascending air sample will change with height in connection with condensation of the water vapour; for descending motion, however, we can consider s to be a constant, and equ. (2, 17) then gives a *parabolic distribution* with height for the vertical velocity. This distribution is certainly more smooth than the actual one, but as in the case of temperature, pressure and geostrophic wind, the essential features are kept in the theoretical representation. A merit of the expressen (2, 17) beyond the form $B(z) \cdot C(x, y, t)$ used in the so-called 2 ½-dimensional models, ELIASSEN (1952), EADY (1952), is that (2, 17) allows for a variable level of maximum velocity, whereas the latter prescribes this level to be independent of x, y and t.

We will now eliminate $\frac{\partial k}{\partial t}$ from (3, 17) by means of (2, 9). In the latter equation the coefficients for $\frac{\partial k}{\partial t}$ and $\mathbf{v}_0 \cdot \nabla k$ differ so little that we may put them equal; solving for $\frac{\partial k}{\partial t} + \mathbf{v}_0 \cdot \nabla k$, we get:

$$\frac{\partial k}{\partial t} + \mathbf{v}_0 \cdot \nabla k = -a\mathbf{v}_0 \cdot \nabla \tau_0 - b\hat{z}\mathbf{v}' \cdot \nabla k \quad (2, 18)$$

where a and b are known functions of $\hat{z}$ and $\left(\frac{1}{\eta}\frac{\partial \eta}{\partial z}\right)_{z=\hat{z}}$. Substituting for $\frac{\partial k}{\partial t} + \mathbf{v}_0 \cdot \nabla k$ in (2, 17), we arrive at:

$$sw = -z\left[a\mathbf{v}_0 \cdot \nabla \tau_0 + \left(b\hat{z} - \frac{z}{2}\right)\mathbf{v}' \cdot \nabla k\right] \quad (2, 19)$$

Except for rather high positive values of $\frac{1}{\eta}\frac{\partial \eta}{\partial z}$, both the coefficients a and b are positive; the former will in general be within the interval 0—$2 \cdot 10^{-4}$ and the latter will mainly keep within the range 1—6. For $\hat{z} = 5$ km b is given by the expression

$$b = \frac{0.72 - 0.25\left(\frac{1}{\eta}\frac{\partial \eta}{\partial z}\right)_{z=\hat{z}} \cdot 10^4}{0.30 - 0.46\left(\frac{1}{\eta}\frac{\partial \eta}{\partial z}\right)_{z=\hat{z}} \cdot 10^4} \quad (2, 20)$$

which is depicted in fig. 1. In general the quantity $\left(b\hat{z} - \frac{z}{2}\right)$ will be positive and since

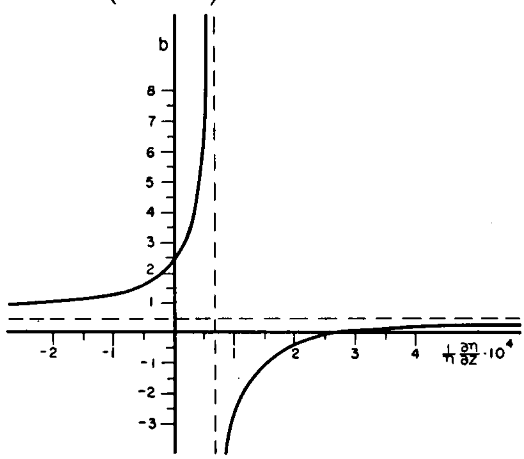

Fig. 1. The quantity b in equation (2, 20) as a function of $\frac{1}{\eta}\frac{\partial \eta}{\partial z}$. The dashed lines are the asymptotes $b = 0.5$ and $\frac{1}{\eta} = 0.64 \cdot 10^{-4}$.

this also applies to a, the coefficients for $\mathbf{v}_0 \cdot \nabla \tau_0$ and $\mathbf{v}' \cdot \nabla k$ in (2, 19) are in most cases negative.

Equation (2, 19) gives a rather interesting relationship between the vertical velocity and the thermal field. This applies especially to the second right hand term which relates the change in direction of the horizontal temperature gradient with height to the vertical velocity. Models sofar applied to numerical forecasting have disregarded this non-parallelism in the temperature gradient along the vertical, but this effect is obviouly important from the standpoint of the termodynamics. Actual computations have shown that the second right hand term in (2, 19) is not only of the same order of magnitude as the first one, but may also become the dominating one.

The relationship expressed by (2, 19) can briefly be summarized as follows:

a) The vertical velocity is proportional to the gradient in τ_0.

b) In the case of uniform lapse-rate ($\nabla k = 0$), the vertical velocity is determined by the sea level temperature advection of the model; warm air advection gives rise to ascending motion and cold air advection gives rise to descending motion.

c) In a region where $\mathbf{v}_0 \cdot \nabla \tau_0 = 0$, a non-vanishing vertical velocity requires that the horizontal temperature gradient changes direction with height; advection of low lapse-rate corresponds to descending motion and advection of high lapse-rate corresponds to ascending motion.

Fig. 2 gives a schematic picture of the case $\mathbf{v}_0 \cdot \nabla \tau_0 = 0$.

In the still more special case $\mathbf{v}_0 = 0$ (centra of highs and lows, hyperbolic points) it appears from equ. (2, 2) page 000 that the term $\mathbf{v}' \cdot \nabla k$ is proportional to the temperature-advection term in the adiabatic equation (2, 1). The sign of the latter has a well known relationship with the rotation of the geostrophic wind with height, ÁRNASON (1942). It is easily shown that in those points of the sea level pressure chart characterized by the condition $\mathbf{v}_0 = 0$, the sign of the vertical velocity can be determined qualitatively from a wind observation along the vertical in accordance with the following rule:

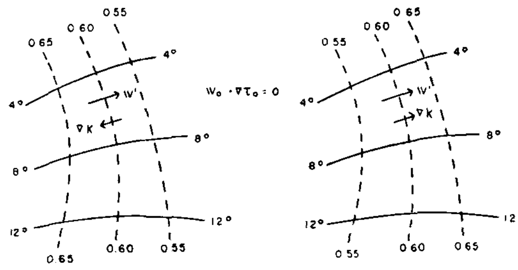

a) Ascending motion b) Descending motion

Fig. 2. The solid lines are isopleths for τ_0, and the dashed lines are isopleths for k. In the case a) there is an advection of high k-values corresponding to ascending motion, in the case b) the advection is the opposite and the motion is a descending one. These results apply only in areas where the sea level temperature advection — $\mathbf{v}_0 \cdot \nabla \tau_0$ — is negligible.

A clockwise rotation of the wind with height (warm air advection) gives descending motion and a counter-clockwise rotation (cold air advection) gives ascending motion.

Remarks on intensity changes of sea level pressure systems. Our third prognostic equation in the form (2, 15) expresses the hydrostatic relationship between the pressure tendency at sea level, the height tendency of the 500 mb surface and the thermal conditions within the layer bounded by these two levels.

Assuming the height tendency of the 500 mb to be known, it is of some interest to study the contribution of this layer to the change in sea level pressure. The last term in (2, 15) is easily interpreted; it is the contribution due to temperature advection at sea level and gives rise to increasing pressure in the case of cold air advection and to decreasing pressure in the case of warm air advection. This term cannot contribute to pressure changes in the centra of lows and highs (deepening, filling). The first term on the right hand side gives the effect of lapse-rate changes, and this term may actually account for intensity changes of a pressure system. Obviously a decrease in the temperature lapse-rate contributes to a pressure fall, and an increase in the lapse-rate contributes to pressure rise.

In order to study alone that part of the thermal effect which is associated with deepening and filling, we will put $\mathbf{v}_0 = 0$. This special case applies to low and high centra and approximately to regions of cyclogenesis.

By making use of (2, 18), equ. (2, 15) is reduced to:

$$\frac{\partial p_0}{\partial t} = -5\, b\hat{z}\mathbf{v}' \cdot \nabla k + 1.1\, \frac{\partial H}{\partial t} \quad (2, 21)$$

where $\hat{z}$ is the height of the level of non-divergence and b is a positive quantity discussed earlier. The first right hand term in (2, 21) is what now is left of the influence of the thermal field upon sea level pressure. It appears quite clearly that non-parallelism with height of the isotherms is closely connected with intensity changes of pressure systems at sea level.

The validity of what has been said above is obviously not restricted by the particular choice of the upper boundary (500 mb surface) of the layer discussed. The latter could just as well have been chosen anywhere within the troposphere. In connection with cyclogenesis it is conceivable that the pressure (height) tendency at some upper tropospheric level is zero, in which case the initiation of the low would be explained exclusively by the rotation of the thermal wind with height.

It is of some interest to quote the following statement made on p. 9 in Technical Report No. 11, "Research on Atmospheric Pressure Changes", published by the Department of Meteorology, Massachusetts Institute of Technology: "Cyclones develop and, therefore, pressure falls are created in regions of strong temperature contrast near the earths surface. However, the development of a particular cyclone is not determined by the magnitude of the temperature contrast. A strong tropospheric temperature gradient is a necessary but not sufficient condition for the development of a new pressure fall". These empirical findings compare well with theory. The theory shows first, that temperature contrast in the troposphere are necessary, and secondly, it distinguishes between cases when the temperature contrast is favourable and when it is not. With reservation on the contribution of the tendency at the upper boundary of the tropospheric layer under consideration, and with reference to the discussion of the term $\mathbf{v}' \cdot \nabla k$ in the section on vertical velocity, one can express the following relationship between cyclogenesis and the rotation of the wind with height:

In a region where $\mathbf{v}_0 \approx 0$, cyclogenesis (deepening) is favoured if the tropospheric wind rotates clockwise with height (warm air advection), the condition being more favourable the stronger the rotation and the stronger the tropospheric temperature gradient. Opposite rotation (cold air advection) is unfavourable for cyclogenesis (deepening), and a strong temperature gradient is adverse in this case. The reverse applies to the strengthening or genesis of an anticyclone.

Returning to equ. (2, 21) where the last term is the 500 mb tendency, it may be seen that the latter is essentially determined by the vorticity advection at this level, since the 500 mb surface coincides approximately with the level of non-divergence. An inspection of the contour pattern of the 500 mb chart may often reveal the approximate position of areas of fall and rise and thus give an idea of the sign of the contribution of the height tendency at this level to eventual cyclogenesis in a certain region. This information together with the rule given above may at least in some cases enable the forecaster to predict qualitatively cyclogenesis and deepening of existing lows.

The stratosphere. So far only the troposphere has been dealt with. Three parameters p_0, τ_0 and k were required for the definition of this part of the model, and three prognostic equations were obtained for the purpose of predicting the changes in these three parameters. One more parameter—the tropopause height h—is needed if the stratosphere is to be included and a forecast for the stratosphere requires a prognostic equation for this quantity. This, *the fourth prognostic equation*, is obtained from the kinematic boundary condition for the tropopause

$$\frac{\partial h}{\partial t} = -\mathbf{v}_h \cdot \nabla h + w_h \quad (2, 22)$$

where the subscript h refers to the tropopause level.

The change in the stratospheric temperature τ_s of the model is determined from the dynamic boundary condition for the tropopause, written in the form:

$$\frac{\partial \tau_s}{\partial t} = \left(\frac{\partial \tau}{\partial t}\right)_{z=h} - k\,\frac{\partial h}{\partial t} \quad (2, 23)$$

Regarding the vertical velocity in the stratosphere, it appears from the adiabatic equation, when applied to the stratosphere, that it remains practically constant with height. This is not believed to be realistic, but an improvement would require one more parameter for describing the stratospheric distribution of temperature. The distribution of the vertical velocity in the stratosphere is not thought to be of primary interest in numerical forecasting and probably does not justify the additional labour involved in a further increase in the number of parameters.

3. Application to a synoptic case

Method of determining the parameters from observations. Before one can apply the prognostic equations derived in the preceding section, the parameters p_0, τ_0, k, and h have to be determined from actual observations. We can obviously put p_0 equal to the observed sea level pressure, thus making sure that the sea level distribution of pressure is correctly given by the model. It is not advisable to do the same with τ_0 because of the lack of representativeness of the observed sea level temperatures. In fact the best procedure for determining the three remaining parameters is not obvious. Generally speaking we have three degrees of freedom in adjusting our model to the atmosphere and we can therefore select three conditions to be fulfilled. We may, for instance, require that the temperature be correctly reproduced at three levels z_1, z_2, and z_3 or that the heights of three selected pressure surfaces be the same in the model as those observed. One of these levels must, however, be in the stratosphere. From a practical point of view the latter alternative would be preferable, but we have still some freedom in selecting the three pressure levels. One of these pressure levels should be close to or within the transition zone between the troposphere and the stratosphere and another near the middle (with regard to pressure) of this one and sea level. The last one should be chosen well within the stratosphere, suitably, at the greatest height reached by the majority of the soundings. As an example the pressure levels 700, 300 and 100 mb could be chosen. In subtropical regions 600, 200 and 100 might be a better choice.

The equations expressing these requirements are not given here since in the case treated below, a somewhat more simple procedure has been chosen. In the first place a forecast for the stratosphere has not been attempted and this allows us to drop the parameter h (tropopause height) of the model. Secondly the following compromise between the two alternatives discussed above has been chosen:

a) k has been put equal to the temperature difference divided by the height difference between the 850 mb and the highest standard pressure level (400, 300, or 200 mb) in the troposphere.
b) τ_0 has been determined by requiring that the thickness of the layer between the 850 mb surface and the upper pressure surface (400, 300 or 200 mb) be correctly given by the model.

The temperature lapse-rate k was computed by a slide rule, whereas τ_0 was determined by means of a graph of the type shown in fig. 3.

The procedure used here neglects entirely the influence of the layer between sea level and the 850 mb surface. In the particular case selected for numerical computations, an inspection of the ascent curves showed that the k-values were very little influenced by this

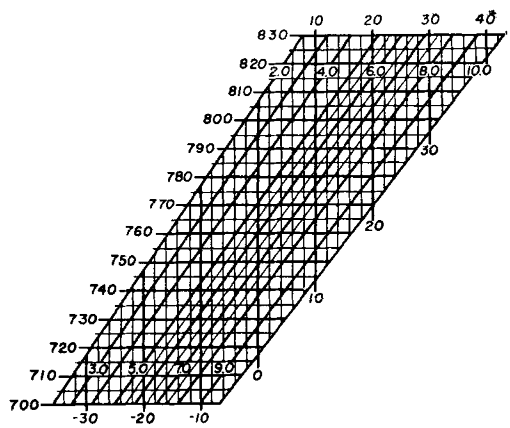

Fig. 3. A graph for determining the temperature at 850 mb in the model atmosphere corresponding to observed mean lapse-rate and observed thickness of the layer 300—850 mb. The slanting lines are those of constant temperature lapse-rate in °C per km, the horizontal lines give the thickness of the 300—850 mb layer in dekameters, and the vertical lines the temperature at 850 mb in °C. *Example:* thickness 755, lapse-rate 6.5, gives 0° C.

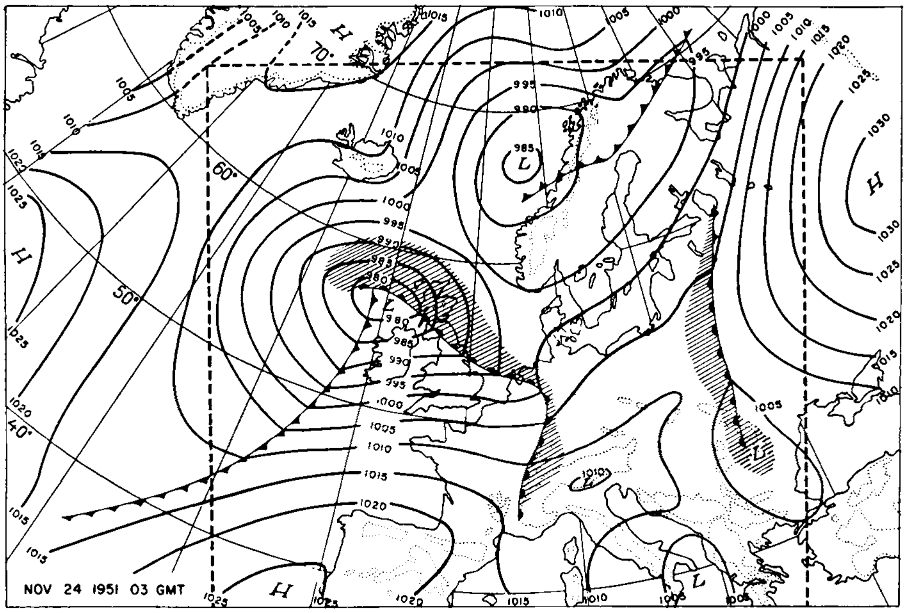

Fig. 4. Sea level pressure chart Nov. 24, 1951 at 03 GMT. The dashed rectangle shows the area of computations.

procedure. As the thermal conditions within this layer may be seriously influenced by non-adiabatic processes and since such effects are not included in the prognostic equations, the forecast is more satisfactorily tested by excluding the influence of this layer.

The synoptic situation. The case used for the numerical computations was the synoptic situation over Western Europe and the Eastern Atlantic on Nov. 24 1951 at 03 z. The synoptic pattern is shown on the sea level chart (fig. 4) and the 500 mb chart (fig. 5). The predominant features at sea level are the high pressure over Greenland and southward over the ocean, and two lows, one centred just west of Scotland and the other off the Norwegian coast. The Scotland low moved from the west and deepened somewhat during the preceding 24 hours, whereas the other one—an old low—had been almost stationary during the same period, but slowly falling pressure to the west of the centre since 18 z of the preceding day indicated slow movement toward the west. It had deepened about 3 mb during the last six hours.

Between these two lows and the high pressure area to the west, a strong cold air outbreak was taking place over the ocean.

The 500 mb chart is dominated by a cold tilted trough extending from the northern edge to the southwestern corner of the map. Another cold trough extends from Scandinavia toward the Adriatic Sea. Isolines (dashed) for absolute vorticity at this level, in units of (60 hour)$^{-1}$, have been superimposed on the chart. There is rather strong advection of vorticity west and southwest of the British Isles, just behind the sea level cold front.

The charts for τ_0 and k are shown on figs. 6 and 7. These are new types of charts—especially the latter—so that previous maps for these elements were not available. In analysing them one therefore did not have the advantage of a continuous series of charts. Fortunately the upper air network within the area of computation (see the dashed rectangle in fig. 4) is sufficiently dense that these charts still can be considered reasonably reliable. Details in the τ_0 distributions over Western France and Scandinavia are, however, somewhat doubtful.

Isolines (dashed) for k (fig. 7) have been superimposed upon the sea level pressure

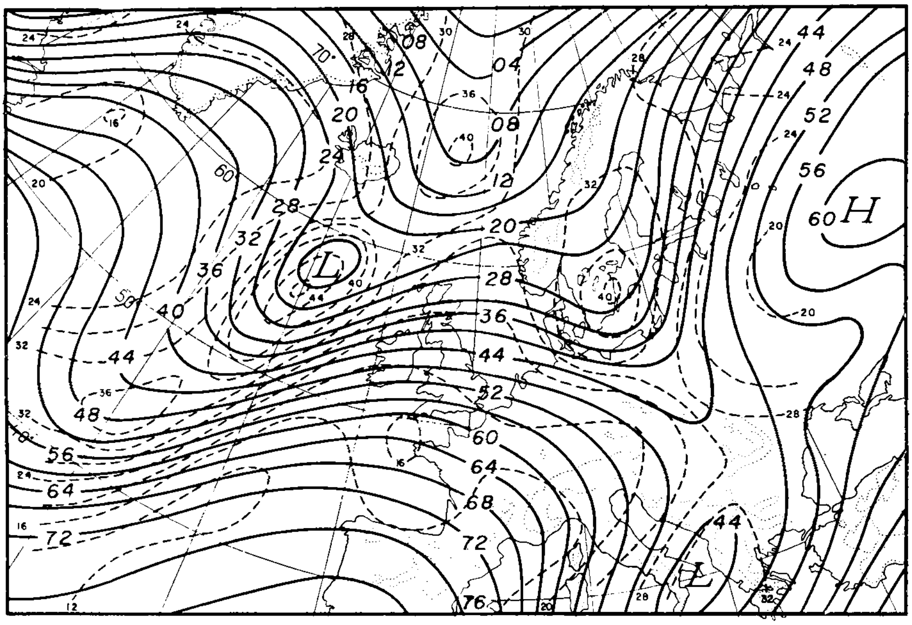

Fig 5. A 500 mb chart for Nov. 24, 1951 at 03 GMT. The dashed lines are the isopleths for absolute geostrophic vorticity at this level. The vorticity figures correspond to a time unit of (60 hours)$^{-1}$.

chart; the unit is °C per km. There is a very pronounced gradient in lapse-rate within the cold air outbreak, and an especially low lapse-rate may be noted behind the central portion of the cold front in the Atlantic. Another noticeable feature is the region of high lapse-rate over Scandinavia.

The distribution of absolute vorticity at sea level and of relative vorticity (dashed lines) are shown in figs. 8 and 9 resp. The units are (60 hours)$^{-1}$.

The grid used for the computations had a mesh-size of 300 km at 45° lat., and the number of points was 14×13. The area, rectangular in shape, is outlined on fig. 4 by dashed lines.

The numerical forecast. Instantaneous changes in k, τ_0 and p_0 have been computed from the prognostic equations (2, 3), (2, 9), and (2, 15). In order to determine the change in p_0 from the last equation quoted, a 500 mb tendency was computed by means of the integrated vorticity equation (2, 12), where the constant γ was assumed to be 0.6.

Fig. 10 shows the computed tendency for k expressed in °C km^{-1} (6 hours)$^{-1}$. The predominant features of this prognostic chart are the fall areas east of Iceland, west of Ireland and over the Baltic Sea. The areas of increase in temperature lapse-rate are much less pronounced. In order to check the results, the 6-hourly observations from 2 British weather ships, 8 upper air stations in Great Britain and 7 in Germany—altogether 17 upper air stations—have been compared with the predicted changes. These stations are shown as dots on the chart, and the figures beside are the observed changes. The arrangement of the figures is explained in the legend of fig. 10. In addition to these 17 stations there are some few upper air stations indicated by crosses; these stations make 12-hourly observations only. The figures beside them show half the observed change from one observation to the next and are arranged in the same manner as the figures beside the dot-stations. On the whole there is a fair agreement between the computed changes and those observed. The strong fall region north-east of Iceland could not be checked directly due to lack of observations, but observed changes in sea level pressure (see later) support indirectly the computed changes in k. The

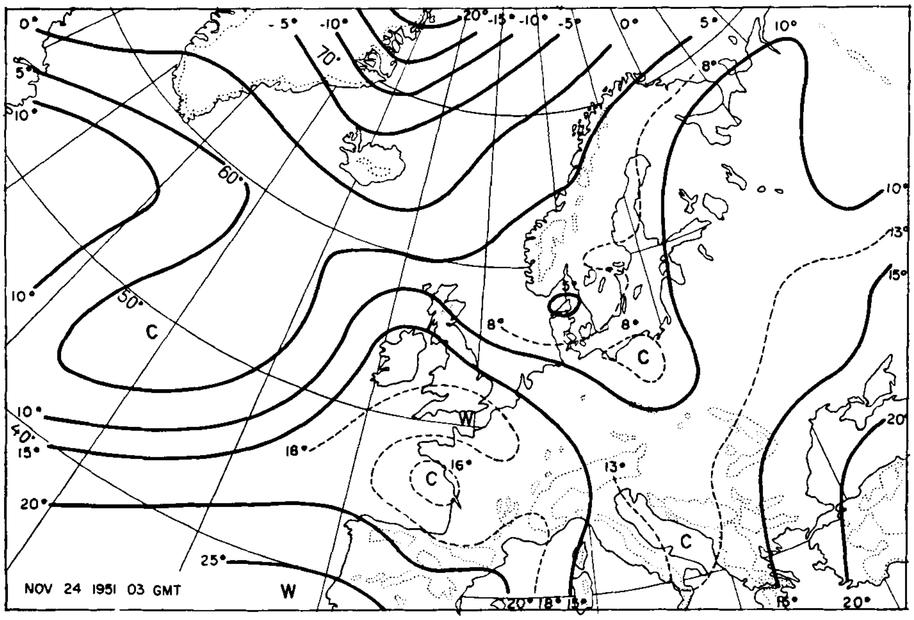

Fig. 6. Isopleths for τ_0 labelled in °C.

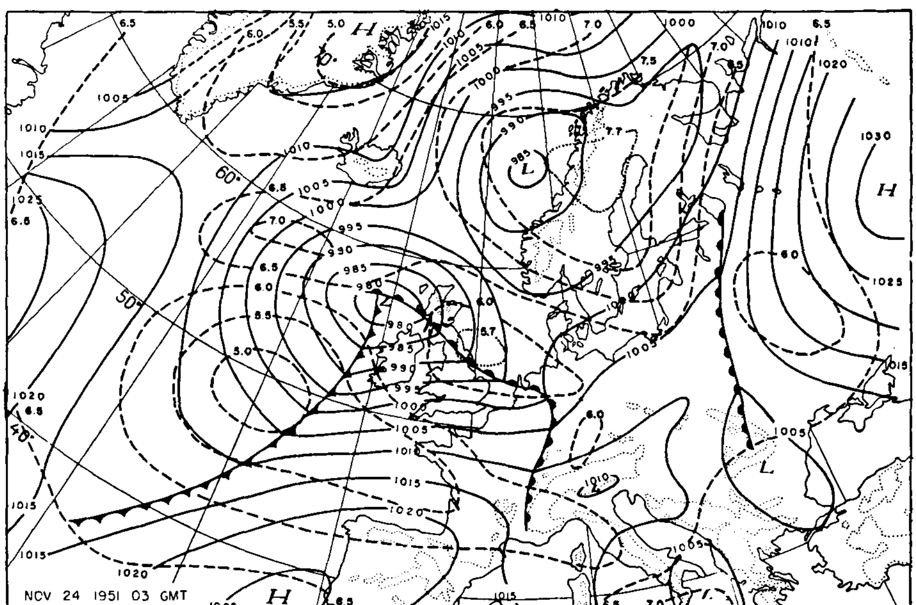

Fig. 7. The dashed lines are isopleths for k labelled in °C per km.

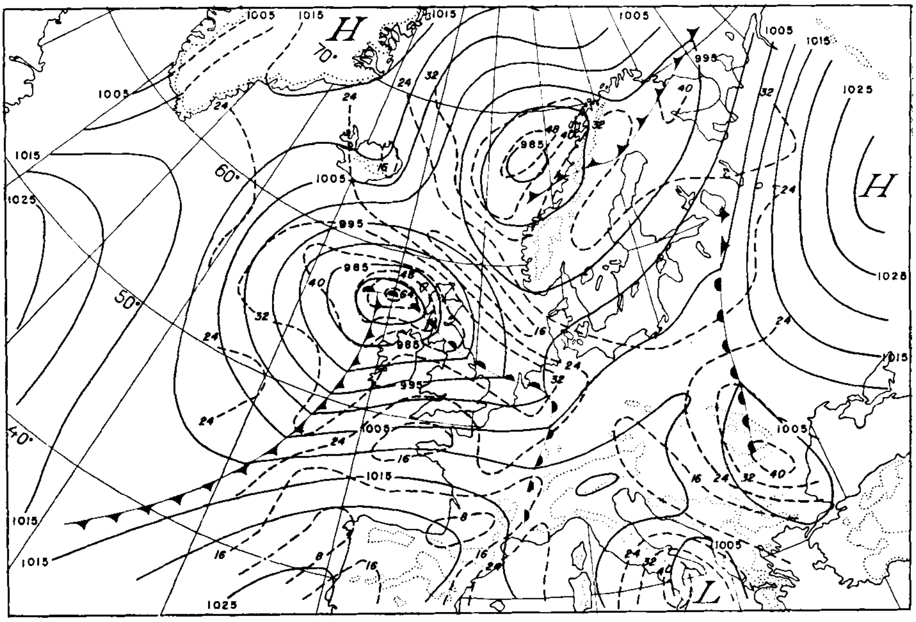

Fig. 8. The dashed lines are isopleths for absolute vorticity at sea level in unit of (60 hours)$^{-1}$.

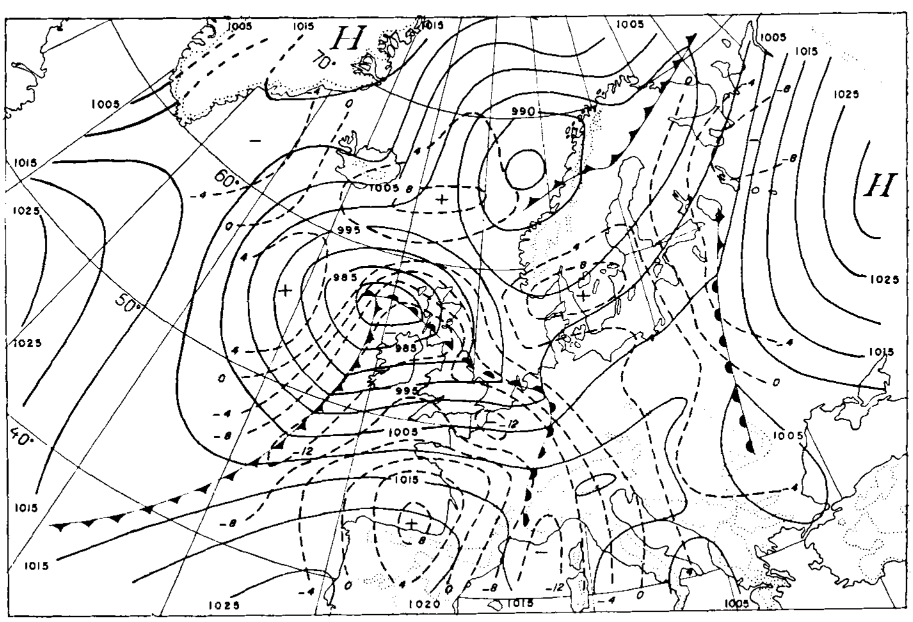

Fig. 9. The dashed lines are isopleths for the relative vorticity for the layer 0—5 km computed from the τ_0 and k maps. The unit is (60 hours)$^{-1}$.

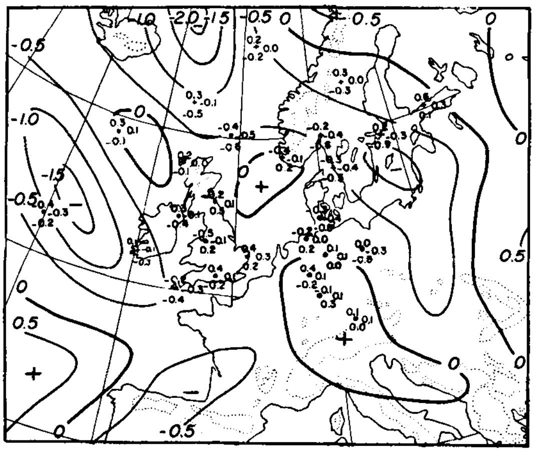

Fig. 10. 24 Nov. 1951 03 GMT. The isopleths give the computed instantaneous change in the tropospheric temperature lapse-rate expressed in °C per km per six hours. The dots indicate stations from which six-hourly observations are available. Of the figures beside the points, the uppermost one is the observed change for the preceding six hours and the lowest one the observed change for the following six hours. The middle figure is half the change for the twelve hours 21—09 GMT. The crosses and the figures beside them refer in a similar way to stations making twelve-hourly observations.

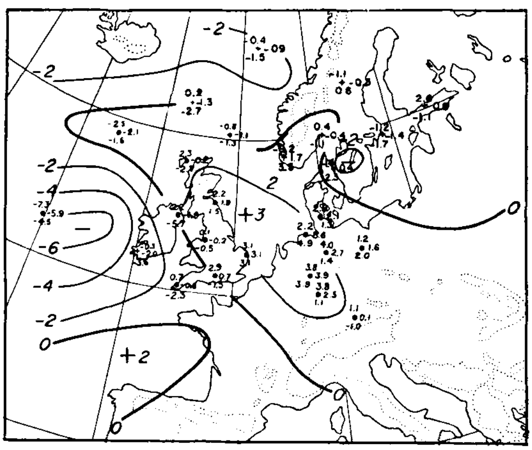

Fig. 11. 24 Nov. 1951 03 GMT. The isopleths give the computed instanteneous change in the surface temperature τ_0 expressed in °C per six hours. Otherwise reference is made to the lapse-rate tendency map.

existence of the negative area with its centre over the Baltic Sea is directly verified by the upper air stations in Southern Scandinavia and indirectly by computed vertical velocities together with the observed state of the sky in this region (discussed later).

Fig. 11 shows the computed distribution of the τ_0 tendencies expressed in °C per six hours. The observed six-hour changes are shown in the same way as on the tendency chart for k. On the whole the computed tendencies are in a good agreement with observations. An exception is the British weather ship at 59° N, where the forecast is in error by about 2°C. An inspection of the charts for τ_0 and p_0 indicate that here the instantaneous temperature advection $\mathbf{v}_0 \cdot \nabla \tau_0$—which essentially determines the change in τ_0—is not representative for a time interval as long as six hours.

In order to obtain the tendencies for the sea level pressure, the 500 mb height changes were first computed and the former thereafter determined from (2, 15). The forecast of the 500 mb changes was rather unsuccessful and this contributes essentially to the discrepancy between the computed sea level pressure changes and those observed, (see table 1). The chart for the computed changes in p_0 is given in fig. 12. The solid lines show the observed change (mb) in sea level pressure from 00—06 z the 24th and the dashed lines the computed tendency expressed in mb per 6 hours. The general pattern is very much the same in both cases, and the dominating fall area over Scotland is fairly well predicted. Regarding the details there are, however, a considerable number of discrepancies, and it is of some interest to attempt an

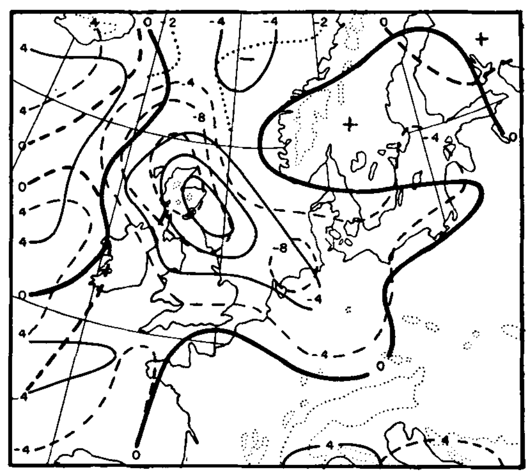

Fig. 12. The solid lines are observed changes in sea level pressure p_0 (mb) from 00—06 z Nov. 24, 1951. Dashed lines represent the computed tendency in the sea level pressure expressed per six hours.

Tab. 1. Observed $\triangle H$ means the observed change in the height (in dekameters) of the 500 mb surface. The 6th column shows the difference in observed change per six hours in H and its computed tendency expressed as change per six hours. Next column shows in the same way the difference in the observed change in p_0 from 00—06 z and the computed change, and in the last one is given the portion of the error in the p_0-forecast which may be attributed to the k, τ_0-forecast.

Station	$(\triangle H)$ observed			$(\triangle H)$ comp.	Mean $(\triangle H)$ obs. minus $(\triangle H)$ comp.	$(\triangle p_0)$ obs. minus $(\triangle p_0)$ comp.	Error from k, τ_0-forecast
	21—03 z	03—09 z	Mean				
Lerwick	—1	—3	—2	—2	0	0 mb	0 mb
Stornoway	—4	—7	—5	—5	0	5	5
Leuchars	1	—9	—4	—3	—1	0	1
Aldergrove	—2	—8	—5	—2	—3	2	5
Liverpool	0	—3	—1	0	—1	2	3
Hemsby	1	3	2	2	0	2	2
Larkhill	1	—2	0	0	0	2	2
Camborne	2	—2	0	—3	3	0	3
59°, 6N, 15°, 6W	—1	—1	—1	0	—1	5	6
52°, 5N, 20°, 0W	—6	—3	—4	1	—5	—3	2
Berlin	2	4	3	—2	5	4	1
Wiesbaden	9	0	5	0	5	3	2
München	0	—2	—1	1	2	2	0
Hamburg	4	4	4	—1	5	4	1
Hannover	4	2	3	—1	4	3	1
Jever	4	5	5	0	5	4	1
Iserlohn	3	6	5	1	4	4	0

analysis of those. We notice in the first place that the computed changes over Western and Northern Europe are 2—4 mb below those observed. This difference is mainly a result of the rather poor 500 mb forecast over this area. The same applies to the interesting fall region in the western part of the old low off the Norwegian coast. This fall was predicted to only around 50 % of the observed values. The predicted fall area over the Baltic Sea is mainly to be attributed to the predicted change in k (see fig. 10); since this fall region is not observed we may infer that the predicted k-distribution is somewhat erraneous or at least not representative for a time interval of six hours. The existence of the two centres of rising pressure near the left edge of the forecast chart is not verified by observation. This discrepancy is at least partly explained by the lack of representativeness in the computed advection term $\mathbf{v}_0 \cdot \nabla\tau_0$ (see equ. (2, 15)) as mentioned previously in connection with the τ_0-forecast.

A feature of special interest is the deepening of the old cyclone off the Norwegian coast. Fig. 13 shows the sea level chart for 12z of the 24th, 9 hours later than the charts upon which the computations are based. The low has deepened about 9 mb and has developed into a cyclone of considerable intensity. The isobar spacing indicates strong winds to the north and west of the centre and surface winds at the coastal stations of Norway have increased from force 3 to 6 Beaufort. As mentioned above, this deepening was not predicted to its full extent. Upon inspection of the three right hand terms of (2, 15) it appears that the deepening may be attributed to the first and second terms, whereas the third one contributes to a pressure rise. The contribution of each of the three terms is roughly equal in magnitude and also approximately equal to the magnitude of the observed pressure fall. Since the height tendency term in (2, 15) is thus approximately cancelled out by the advective term, the deepening of the old cyclone cannot be explained without the first term, i.e. in this case *the change in intensity was essentially connected with the non-uniformity in the horizontal temperature lapse-rate.*

On the whole the computations shows that the term $5\,\frac{\partial k}{\partial t}$ in (2, 15) is, in the synoptic situation treated here, comparable in magni-

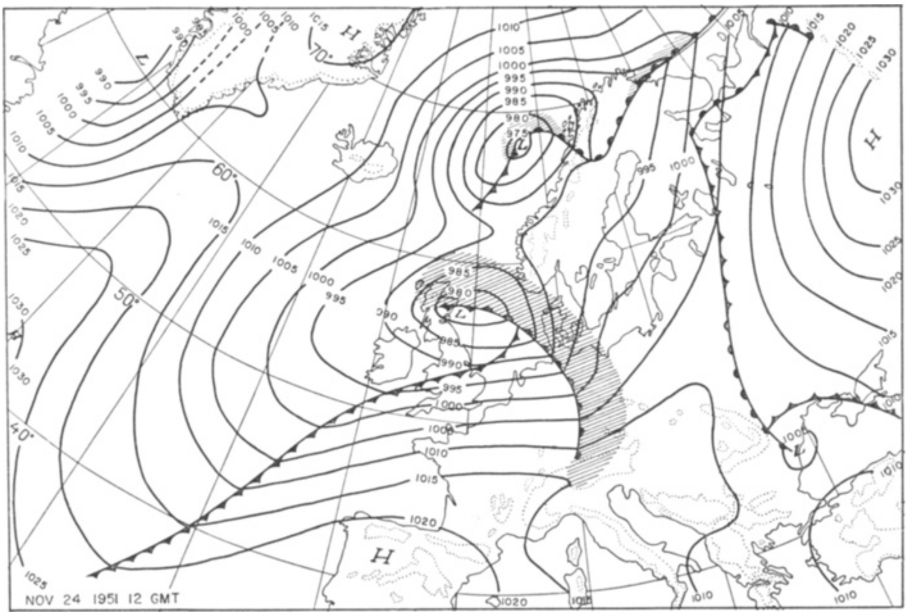

Fig. 13. Sea level pressure chart Nov. 24, 1951 at 12 GMT.

tude with the two other right hand terms, thus verifying the importance of horizontal gradients in temperature lapse-rate as advocated in the theoretical considerations.

It may be worth while to mention that the greatest computed values of the first, second and third right hand terms of (2, 15) were 10, 5 and 14 mb respectively.

Table 1 shows the observed changes in the height of the 500 mb level over the 17 stations mentioned earlier. The computed changes are found in column 5 and the differences between the observed and computed changes are given in the 6th column. The 7th shows the differences between observed and computed changes (in mb) for the sea level pressure, and the last column the portion of error in the p_0 forecast, for each station, attributed to error in the forecast of τ_0 and k. These errors are greatest for Stornoway, Aldergrove and the weather ship at 59°,6 N, 15°,6 W; it appears from the p_0, τ_0 maps that this depends, to some extant at least, on the lack of representativeness of the computed values of temperature advection at these stations during the succeeding six hours.

The distribution of computed vertical velocity at 5 km, obtained by use of (2, 19), is shown in fig. 14. The dashed lines are isopleths labelled in cm/sec. On the whole the picture of the vertical velocity distribution seems reasonable as judged from the synoptic situation. The strong subsidence in the cold air outbreak and the ascending motion ahead of the warm front are in good agreement with our general experience. It should be mentioned that in the computations the dry-adiabatic lapse-rate has been used for k_a in the expression $s = k_a - k$ in the equation for vertical velocity. In a region of ascending motion this will not hold true when condensation takes place, and one should preferably use the saturation adiabatic lapse-rate. This has roughly been taken into account by doubling the computed velocity figures in areas of ascent. The doubled figures are shown in brackets following the computed figures.

The vertical velocity pattern cannot be checked directly by observations, but cloud reports give some indication as to whether the distribution is reasonable or not. At 06 z, stations within the cold air outbreak report alternately some showers (present and past) or cumulus cloud but the amount of cloudiness is less than 5/10 and no other clouds are reported. Because of considerable non-adiabatic

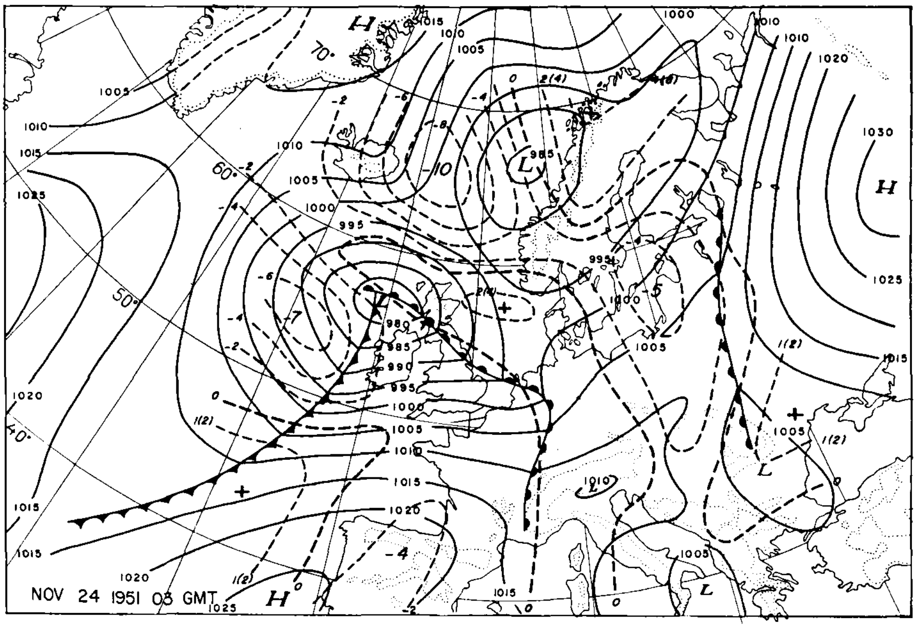

Fig. 14. The dashed lines give the vertical velocity in cm/sec at 5 km. The figures in brackets in the regions of ascending motion correspond roughly to a saturation-adiabatic change in the temperature of a rising particle. Otherwise the dry-adiabetic temperature change has been used.

heating of the cold air while traversing the warmer sea, it is conceivable that such showers may develop in spite of general subsidence.

The region of subsidence centred over the Baltic Sea is supported by the cloudless skies at a number of stations in eastern Sweden, whereas the overcast sky over the costal region of the Lathaunia, Latvia and Estonia indicates that this subsidence area may be overestimated in the computations. The area of ascending motion over northern Scandinavia is indirectly verified by the overcast sky and some precipitation reported at 06 z. Finally, reports of rain and overcast sky from ships in the Atlantic support the computed vertical motion west of Portugal.

Acknowledgment

The author wishes to express his thanks to Professor C.-G. Rossby for his encouragement during the course of this work including the previous paper of the same title. Thanks are also extended to staff members and visitors of the Institute of Meteorology, University of Stockholm, for valuable discussions.

Most of the numerical calculations in both papers have been carried out by one of the technical staff members, B. Johnsson, to whom the author wishes to express his sincere thanks.

REFERENCES

ÁRNASON, G., 1942: Distribution of mass variations in atmospheric air columns. *Meteorologiske Annaler*, **1**, 10.

ÁRNASON, G., 1952: A baroclinic model of the atmosphere applicable to the problem of numerical forecasting in three dimensions. I. *Tellus*, 4, 4.

EADY, E. T., 1952: Note on weather computing and the so-called $2^1/_2$-dimensional model. *Tellus*, **4**, 3.

ELIASSEN, A., 1952: Simplified dynamic models of the atmosphere designed for the purpose of numerical weather prediction. *Tellus*, **4**, 3.

FJØRTOFT, R., 1952: On a numerical method of integrating the barotropic vorticity equation. *Tellus*, **4**, 3.

Massachusetts Institute of Technology, Technical Report No. 11, 1952: Research on atmospheric pressure changes.

THOMPSON, P. D., 1952: Notes on the theory of large-scale disturbances in atmospheric flow with application to numerical weather prediction. *Geophysical Research papers No.* **16**, Air Force Cambridge Research Center.